e-ISSN: 2550-164X

Available online at
https://jmeche.uitm.edu.my/

Journal of Mechanical Engineering 22(1) 2025, 79 – 89.

Journal of Mechanical Engineering

Distortion Behaviour Analysis of Additively Manufactured Inconel 718 using Numerical Computation

Azri Rahimi Abd Rahman[1], Nor Asiah Muhammad[2], Muhd Faiz Mat[1*], Yupiter HP Manurung[1], Mohd Shahriman Adenan[1], Yusuf Olanrewaju Busari[1,3], Keval Priapratama Prajadhiana[1], Turnad Lenggo Ginta[4], Triyono[5]

[1]*Smart Manufacturing Research Institute, School of Mechanical Engineering, College of Engineering, UiTM Shah Alam, Selangor Darul Ehsan, Malaysia*
[2]*Politeknik Premier Sultan Salahuddin Abdul Aziz Shah, Malaysia*
[3]*Materials & Metallurgical Engineering Department, University of Ilorin, Ilorin, PMB 1515, 230001, Nigeria*
[4]*Research Centre for Manufacture and Industrial Process Technology, Banten, Indonesia*
[5]*Mechanical Engineering Department, Universitas Sebelas Maret, Surakarta, Indonesia*

ARTICLE INFO

Article history:
Received 18 June 2024
Revised 10 August 2024
Accepted 13 September 2024
Online first
Published 15 January 2025

Keywords:
Metal additive manufacturing (MAM)
Direct energy deposition (DED)
Distortion
Simulation
Inconel 718

DOI:
10.24191/jmeche.v22i1.2801

ABSTRACT

Metal Additive Manufacturing (MAM) is a rapidly growing technology that has the potential to revolutionize the manufacturing industry. One of the current MAM processes is direct energy deposition (DED), which uses layer-by-layer deposition to design for part consolidation and minimize materials wastage. However, repeated heating and cooling of the DED process often exhibit distortions in AM components, leading to premature failure. The study presents the numerical computation analysis of the thermally induced distortion of additively manufactured Inconel 718 on SS316 substrate utilizing the DED process with the help of numerical computation software Simufact Welding. The geometry design of the Inconel 718 component and SS316 substrate is designed to establish a deeper understanding of the LMD process's distortion behaviour. The simulation results show that the distortions increase with the number of layers, and the distortion rate varies along the deposition height. Deformation of the substrate at nodes S3 and S5 increased linearly in each of the deposited layers, but the rate decreased at nodes S1 and S2 during the last four layers suggesting temperature uniformity between the substrate and the deposited material.

INTRODUCTION

The fundamental of the additive manufacturing (AM) process is the process of joining material to create a three-dimensional object layer upon layer by slicing the 3D model data. Modern AM technologies have utilized various materials such as polymers, ceramics, and metals to manufacture products (Nazir et al., 2023). Metal additive manufacturing (MAM) has shown to be one of the prominent impacts in the industries

[1*] Corresponding author. *E-mail address*: muhdfaizmat@uitm.edu.my
https://doi.org/10.24191/jmeche.v22i1.2801

(Armstrong et al., 2022). The MAM process uses a heat source to heat metal powder or wire to form an object. Direct energy deposition (DED) is one of the several categories of AM technologies according to ISO/ASTM 52900:2021 that uses powders as feedstock and either laser, arc, or electron beam as the heat source. Laser metal deposition (LMD) directs the laser energy as a light source to produce a tiny melt pool onto the substrate, where metal powder is deposited simultaneously. The powder is then heated, solidified, and forms a new layer on the substrate (Ahn, 2021). Due to a narrow heat-affected zone, the relations of a laser with powder-fed metal in DED offers benefits over conventional processes such as welding and casting (Wolff et al., 2019). Although most of MAM has solved the limitation of the subtractive manufacturing process in design challenges, the uprising technologies have faced difficulty mitigating distortion due to rapid heating and cooling between deposited material and substrate.

Parts distortion developed during the deposition is a major problem hindering the MAM process's adoption on an industrial scale. Hence, a few studies have attempted to understand the development of distortion in AM components. Dunbar et al. (2016) used variable reluctance transducer displacement sensors to record the substrate distortions in the selective laser melting (SLM) process. Afazov et al. (2021) and Ning et al. (2020) have relied on mathematical models for distortion predictions in AM, just as Wacker et al. (2021) employed an artificial neural networks approach to forecast distortions in wire arc additive manufacturing (WAAM). Instead of using in-situ measurement or finite element method (FEM), other investigations use coordinate measuring machines to quantify the distortions of the manufactured components (Ghasri-Khouzani et al., 2017; Yakout et al., 2020).

Besides the experimental study conducted by other researchers, the FEM is necessary within the product development paradigm of the MAM process (Ahmad et al., 2022; Mat et al., 2020). In order to monitor and forecast distortions, Biegler et al. (2022) employed a digital image correlation system, FEM, and numerical models. Prajadhiana et al. (2023) have developed a practical procedure of numerical computation for twenty-five layers of deposition of WAAM on top of a thin plate based on actual experimental results in predicting distortion. Taufek et al. (2022) used FEM software to investigate the inherent strain method (ISM) in forecasting the distortion of SLM specimens.

In this paper, Inconel 718 has been proposed as the study material. Ni-based alloys are frequently utilized as deposit material to increase a product's surface yield strength, ultimate tensile strength, wear resistance, and corrosion resistance. Due to its elevated temperature yield strength and corrosion resistance, Inconel 718 has several uses as turbine components (Reed & Rae, 2014).

In previous research, there is little study of numerical computation investigating the distortion induced by the LMD of Inconel 718. As a result, the discovered insights from this extensive simulation analysis are thoroughly addressed for the additively manufactured Inconel 718. The schematic in Fig 1 shows the distortion developed from the LMD process which occurs in two phases. The newly deposited material exhibits a quick increase in temperature, reaching its melting point. The elevated temperature facilitates the material's expansion, whereas the substrate's reduced temperature constrains its expansion. This phenomenon results in a brief distortion of a convex shape. The process involves transmitting heat from the solidified layer to the substrate by conduction. During the heat transferred from the solidified layer on a substrate, the layer undergoes contraction due to the elevated temperature of the substrate which hinders the contraction process, leading to a permanent concave distortion (Special Metals Corporation, 2021).

Fig. 1. The schematic diagram of distortion during the LMD process.

https://doi.org/10.24191/jmeche.v22i1.2801

METHODOLOGY

Development of numerical computation process

In order to analyse the LMD process of the numerical computation in predicting the distortion behaviour of additively manufactured Inconel 718, the numerical simulation analysis is explored using Simufact Welding. The DED module included inside Simufact Welding has the capability to simulate and assess several factors, such as stress, strain, distortion, temperature history, and hot spots during the production and post-processing stages of DED models. The LMD process is replicated in the DED module from CAD modelling to the process parameters.

The module uses a FEM that neglects the consideration of melt pool convections, instead of prioritizing heat conduction analysis. The deposition of metal in the DED module is simulated as a singular entity due to single-pass welding. Therefore, the meshes linked to the simulation are first set to function in a state of quiet or inactive. Upon initiation of the simulation, the activation of each mesh would take place element-wise using the moving volumetric heat source. During the propagation of the heat source, the elements that come into touch with it undergo permanent activation via the use of an algorithm for element birth. It is essential to acknowledge that the program does not imitate powder deposition. Before conducting the LMD process simulation, it is essential to define the suitable boundary conditions inside the Simufact Welding program. These include defining the mechanical boundary conditions for clamping and bearing. Fig 2 illustrates the dimensions of the geometrical model and the mechanical boundary conditions.

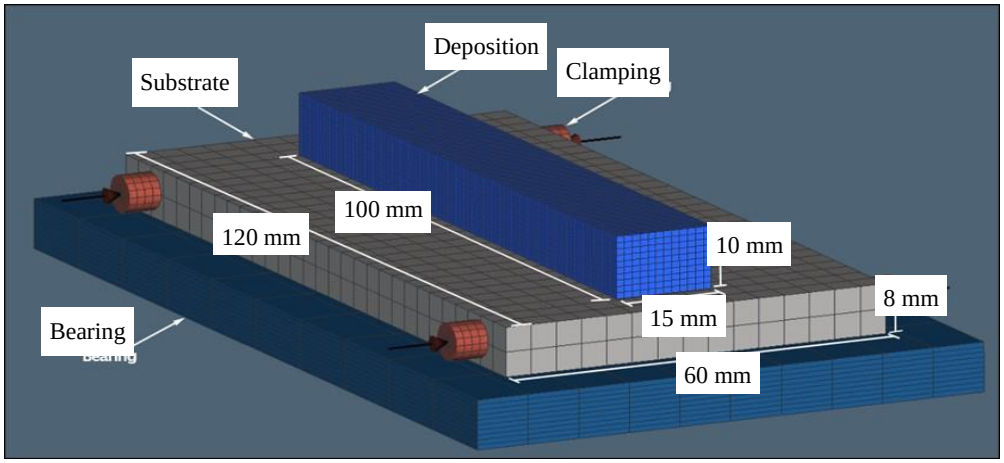

Fig. 2. Geometrical model with dimensions and mechanical boundary conditions of the LMD process.

The objective of the simulation is to deposit a cuboid made of Inconel 718 with the dimensions of 100 × 15 × 10 mm on the SS316 substrate and a thickness of 8 mm. Fig 3 shows a total of 120 trajectories with moving heat sources are assigned to simulate 12 single tracks and a total of 10 layers, with each layer having a 1 mm thickness. The hatch distance of the trajectories is 1.25 mm. The unidirectional deposition strategy is employed, shown in Fig 3, to produce simplicity and load into the DED module in order to construct the geometric structure of the component.

https://doi.org/10.24191/jmeche.v22i1.2801

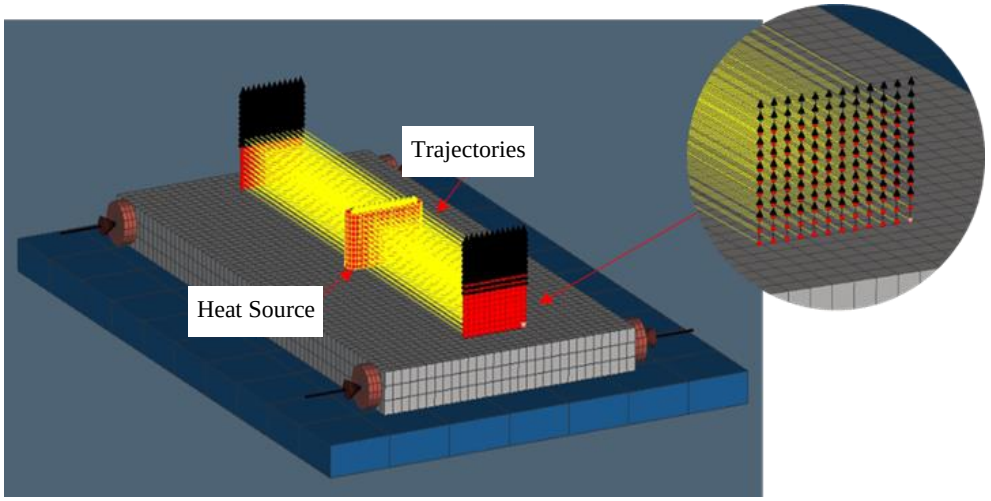

Fig. 3. The total of 120 trajectories of the LMD process and heat sources model used in the Simufact Welding.

The heat source used in the simulation has a cylindrical shape, characterized by a radius of 2.05 mm and a depth of 1 mm. Additionally, the heat source is described by a Gaussian parameter of 0, giving a constant distribution and possessing an absorption efficiency of 66%. The laser spot size diameter is assigned to be 4.1 mm.

The deposited Inconel 718 and SS316 substrate materials need to be designated for creating the numerical model. Prior to the simulation, Table 1 and Table 2 show the nominal composition of Inconel 718 and SS316 obtained with the temperature-dependent material properties shown in Fig 4. The material properties for Inconel 718 such as thermal conductivity, thermal expansion coefficient, specific heat capacity, and Young's modulus were sourced from the Simufact Material database with reference data obtained from the Special Metals technical bulletin for Inconel 718 (Special Metals Corporation, 2021). For material SS316, the mentioned material data in Simufact Material was obtained from other research work (Abburi Venkata et al., 2016).

Table 1. Chemical composition of the SS316 in weight % derived from Simufact Material

	C	Co	Cr	Mn	Mo	N	P	S	Si
SS316	0.018	0.19	16.63	1.57	2.05	0.0153	0.04	0.002	0.48

Table 2. Chemical composition of the Inconel 718 in weight % derived from Simufact Material

	Al	Cr	Mn	Mo	Nb	Ni	S	Si	Ta	Ti	V	W	Zr	C	Co	Fe
Inconel 718	0.8	17.96	0.05	2.64	4.59	56.52	0.006	0.06	0.02	0.87	0.014	0.013	0.016	0.02	0.05	Balance

Table 3 shows the LMD parameters employed in the study. Besides the deposition strategies and materials properties, the chosen input parameters of laser power, scanning speed, and laser spot diameter significantly affect the quality of the product fabricated by the LMD process (Gullipalli et al., 2022a; Gullipalli et al., 2022b; Gullipalli et al., 2022c). The results of the previous study show that these parameters used have successfully minimized the porosity and crack-free of the additively manufactured Inconel 718 component. However, in this study, the parameters chosen are used to investigate the distortion behaviour caused by the repeated heating of the LMD process based on the thermal history in numerical computation analysis.

https://doi.org/10.24191/jmeche.v22i1.2801

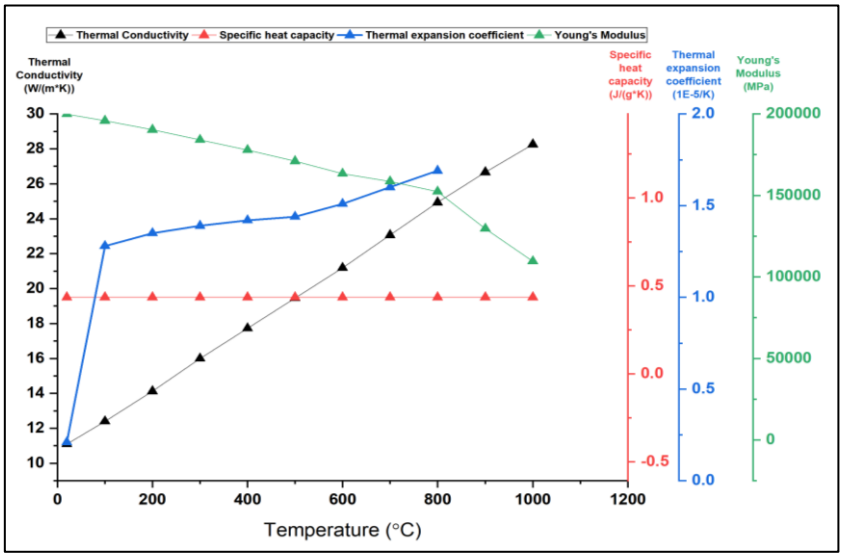

(a)

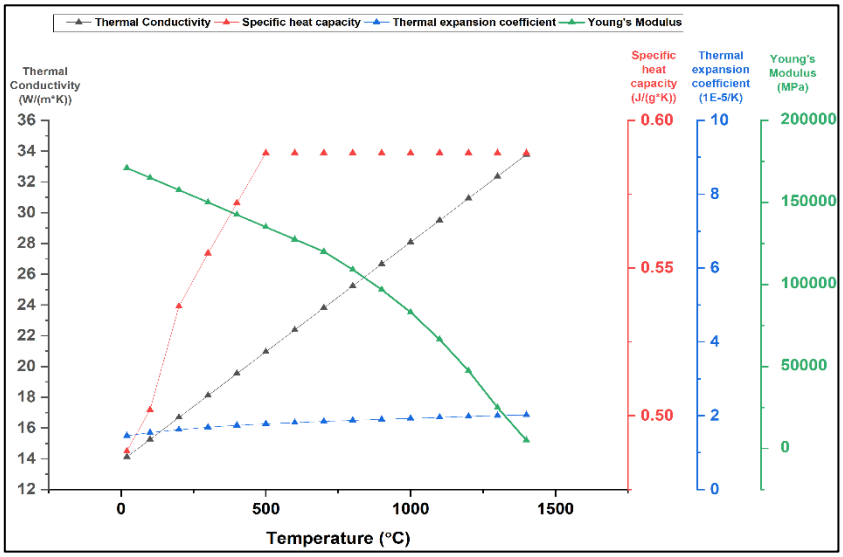

(b)

Fig. 4. (a) Material temperature-dependent properties of Inconel 718 for deposited and (b) SS316 for substrate material derived from Simufact Material.

Table 3: LMD simulation parameters used in Simufact Welding

LMD parameters	Value
Laser power [kW]	2.10
Scanning speed [mm/s]	16.67
Laser spot diameter [mm]	4.10

https://doi.org/10.24191/jmeche.v22i1.2801

RESULT AND DISCUSSION

To obtain the distortion value of the substrate in the software, measurement points are assigned to the geometrical model to compare the initial and final state of the LMD process of the component. A total of 5 nodes (S1-S5) are assigned in the study to monitor and record the distortion at the substrate bottom, and a single node in each layer of deposited Inconel 718 to record the thermal history.

In observing the results of the contour band display obtained in measuring the distortion of the LMD process, Fig 5 shows the highest distortion or maximum displacement of the components that are presented by red and orange colour, in which all corners of the substrate are deflecting upwards and gradually to the blue colour to depict minimum distortion. The theory of distortion of the LMD process is further found to be similar to the simulation.

Fig 6 shows the displacement of nodes and the results of distortion at the bottom of the substrate. The results show that all the assigned nodes experience deformation, with the highest distortion recorded at node S2, which is 2 mm. It should be noted that at the center of the substrate, the distortion should be deflected downward due to concave formation. Instead, minimal distortion is observed at the S4 with 0.2 mm displacement due to the substrate being placed on top of the bearing, preventing the substrate's center from deflecting downwards.

Fig 7 shows a melt pool temperature history of 10-layer deposition recorded in the simulation. The graph shows repeated heating and cooling throughout the deposition with an elevated temperature >1700 °C in each layer.

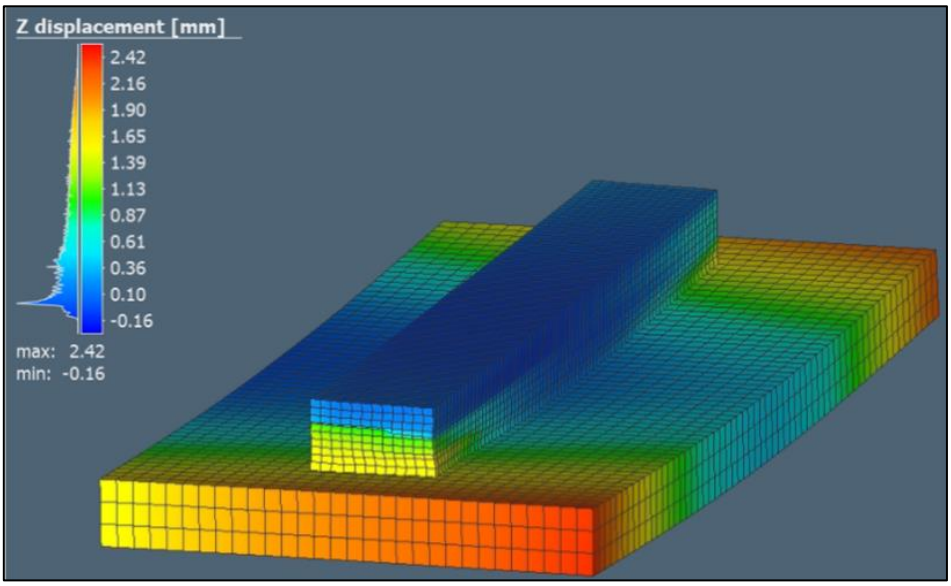

Fig. 5. The color contour results show the variation in distortion around the substrate.

https://doi.org/10.24191/jmeche.v22i1.2801

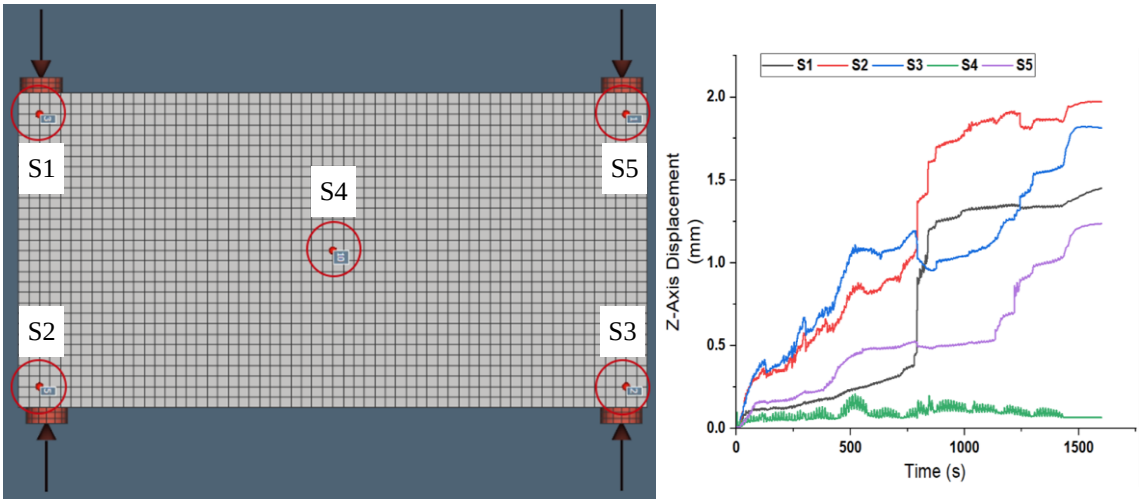

(a) (b)

Fig. 6. (a) The mesh model of the back substrate with marked nodal position and (b) Distortion result of 5 nodes in z-axis displacement.

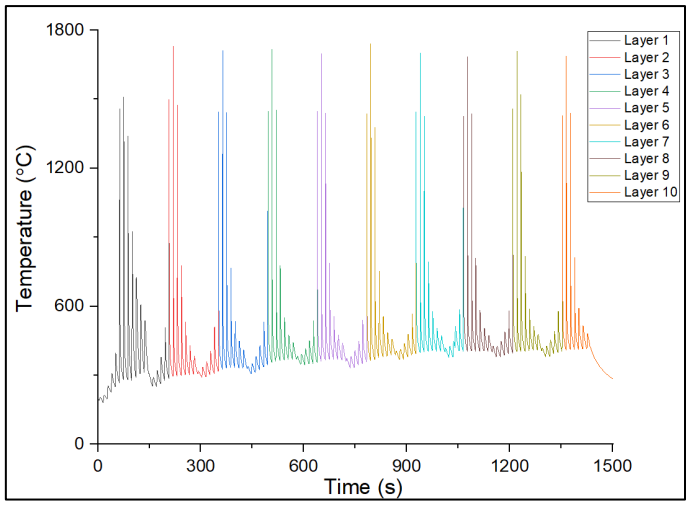

Fig. 7. Thermal history of repeated heating and cooling of deposited Inconel 718 on SS316 substrate.

A cooling rate of 756 °C/s is observed at the peak temperature of the ninth layer during the simulation as shown in Fig 8. The heat cycles experienced during the LMD process result in significant thermal stresses inside the fabricated components.

https://doi.org/10.24191/jmeche.v22i1.2801

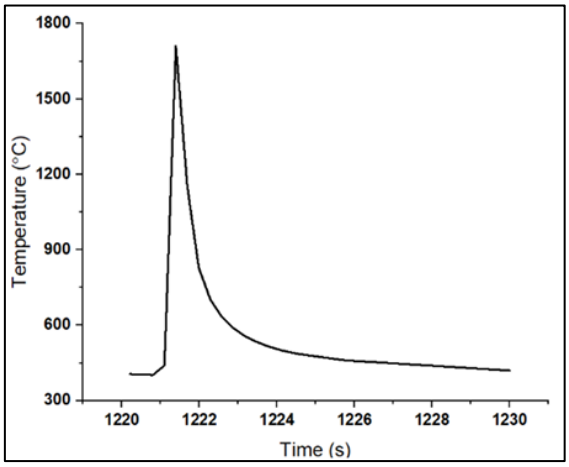

Fig. 8. A cooling rate of 756 °C/s is at the peak temperature of the ninth layer.

Fig 9 shows the thermal history at the bottom of the substrate recorded during the whole deposition. It is worth noting that the highest temperature attained at the bottom surface of the substrate is 374 °C. Based on the data shown in Fig 7 and Fig 8, it can be noted that a significant temperature discrepancy exists between the top and bottom surfaces of the substrate. The temperature data presented provides evidence of significant localized heating, which has the potential to induce plastic deformation in nearby areas. A linear increase of deformation was observed according to the number of layers deposited. Related to Fig 6, the rate of deformation was decreased at nodes S1 and S2 for the 4 last layers suggesting the substrate's temperature had already been uniform with the temperature of the deposited. Furthermore, the quick fluctuation in temperature does not provide enough time to accommodate the plastic deformations occurring in the components that make the LMD component deformed. At nodes S3 and S5, a linear increase of deformation is observed compared to S1 and S2 with uneven deformation rates between those locations suggesting uneven temperature distribution across the substrate due to the unidirectional deposition strategy (Novelino et al., 2022).

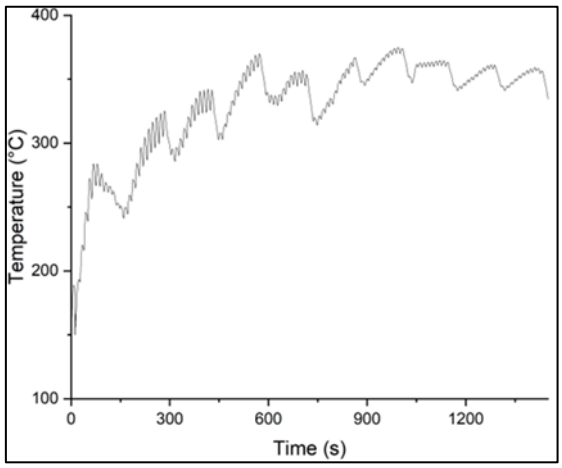

Fig. 9. The bottom temperature of the substrate.

https://doi.org/10.24191/jmeche.v22i1.2801

CONCLUSION

This research has the main objective, which is to analyse the distortion behaviour of additively manufactured Inconel 718 by the LMD process. The study case for this investigation is Inconel 718 cuboid deposited layer upon layer on SS316 substrate in the form of a 12-string, 10-layered LMD process which is modelled with simplified rectangular mesh geometry and simulated with laser heat source model. The contributions from this study can be summarized as follows:

(i) The numerical computation for twelve-string and ten-layer deposition of the LMD process has been successfully simulated using Simufact Welding. The geometrical and process parameters are defined clearly to achieve the desired results.

(ii) The distortion results obtained from the simulation further approve the theory of the distortion behaviour of the LMD process, where the LMD components will form a concave shape due to the elevated temperature of the substrate hindering the contraction of the newly solidified layer.

(iii) The material modelling with JMatPro software will be considered towards further development of this research to compare the accuracy of the simulation and experimental results.

(iv) The in-situ LMD parameters of the experiment can be used in the simulation of the upcoming study to develop a virtual testing of the LMD process.

ACKNOWLEDGMENT

The authors would like to express their gratitude to Fundamental Research Grant Scheme (FRGS) entitled Correlation Between Mechanical Properties, Fatigue Strength and Grain Morphology of Austenitic Stainless Steel (SS316L) Produced by Wire-Arc Additive Manufacturing (WAAM) (FRGS/1/2022/TK10/UITM/02/84) from the Ministry of Higher Education (MOHE) in Malaysia, the staff member of Smart Manufacturing Research Institute (SMRI) as well as the staff of Welding Laboratory, Advanced Manufacturing Laboratory, Advanced Manufacturing Technology Excellence Centre (AMTEx) and Research Interest Group: Advanced Manufacturing Technology (RIG:AMT) at Faculty of Mechanical Engineering, Universiti Teknologi MARA (UiTM). This research is financially supported by College of Engineering, UiTM

CONFLICT OF INTERESTS

One of the authors, Muhd Faiz Mat is a section editor of the Journal of Mechanical Engineering (JMechE). The author has no other conflict of interest to note.

CONTRIBUTIONS OF AUTHORS

The authors confirm their contribution to the paper as follows: **study conception and design**: Mohd Shahriman Adenan, Yusuf Olanrewaju Busari; **data collection**: Keval Priapratama Prajadhiana, Turnad Lenggo Ginta, Triyono; **draft manuscript preparation**: Azri Rahimi Abd Rahman, Nor Asiah

https://doi.org/10.24191/jmeche.v22i1.2801

Muhammad; **supervision**: Muhd Faiz Mat; **resources**: Yupiter HP Manurung. All authors reviewed the results and approved the final version of the manuscript.

REFERENCES

Abburi Venkata, K., Truman, C. E., Smith, D. J., & Bhaduri, A. K. (2016). Characterising electron beam welded dissimilar metal joints to study residual stress relaxation from specimen extraction. International Journal of Pressure Vessels and Piping, 139–140, 237–249. https://doi.org/10.1016/j.ijpvp.2016.02.025

Afazov, S., Semerdzhieva, E., Scrimieri, D., Serjouei, A., Kairoshev, B., & Derguti, F. (2021). An improved distortion compensation approach for additive manufacturing using optically scanned data. Virtual and Physical Prototyping, 16(1), 1–13. https://doi.org/10.1080/17452759.2021.1881702

Ahmad, S. N., Manurung, Y. H. P., Adenan, M. S., Yusof, F., Mat, M. F., Prajadhiana, K. P., Minggu, Z., Leitner, M., & Saidin, S. (2022). Experimental validation of numerical simulation on deformation behaviour induced by wire arc additive manufacturing with feedstock SS316L on substrate S235. International Journal of Advanced Manufacturing Technology, 119(3-4), 1951–1964. https://doi.org/10.1007/s00170-021-08340-4

Ahn, D. G. (2021). Directed Energy Deposition (DED) process: State of the art. International Journal of Precision Engineering and Manufacturing - Green Technology, 8(2), 703-742. https://doi.org/10.1007/s40684-020-00302-7

Armstrong, M., Mehrabi, H., & Naveed, N. (2022). An overview of modern metal additive manufacturing technology. Journal of Manufacturing Processes, 84, 1001–1029. https://doi.org/10.1016/j.jmapro.2022.10.060

Biegler, M., Elsner, B. A. M., Neubauer, I., Lemke, J., & Rethmeier, M. (2022). Result quality evaluation of Directed Energy Deposition Additive Manufacturing simulations with progressive simplification of transient heat-source motion. Procedia CIRP, 111, 277–281. https://doi.org/10.1016/j.procir.2022.08.021

Dunbar, A. J., Denlinger, E. R., Heigel, J., Michaleris, P., Guerrier, P., Martukanitz, R., & Simpson, T. W. (2016). Development of experimental method for in situ distortion and temperature measurements during the laser powder bed fusion additive manufacturing process. Additive Manufacturing, 12(A), 25–30. https://doi.org/10.1016/j.addma.2016.04.007

Ghasri-Khouzani, M., Peng, H., Rogge, R., Attardo, R., Ostiguy, P., Neidig, J., Billo, R., Hoelzle, D., & Shankar, M. R. (2017). Experimental measurement of residual stress and distortion in additively manufactured stainless steel components with various dimensions. Materials Science and Engineering: A, 707, 689–700. https://doi.org/10.1016/j.msea.2017.09.108

Gullipalli, C., Thawari, N., Burad, P., & Gupta, T. V. K. (2022a). Influence of normalized enthalpy on Inconel 718 morphology in direct metal deposition. Proceedings of the Institution of Mechanical Engineers, Part E: Journal of Process Mechanical Engineering, 0(0), 1-10. https://doi.org/10.1177/09544089221116167

Gullipalli, C., Thawari, N., Burad, P., & Gupta, T. V. K. (2022b). Parametric effect on the microstructure of direct metal deposited Inconel 718. Materials and Manufacturing Processes, 37(10), 1165–1174. https://doi.org/10.1080/10426914.2021.2006219

https://doi.org/10.24191/jmeche.v22i1.2801

Gullipalli, C., Thawari, N., Chandak, A., & Gupta, T. (2022c). Statistical analysis of clad geometry in Direct Energy Deposition of Inconel 718 single tracks. Journal of Materials Engineering and Performance, 31(8), 6922–6932. https://doi.org/10.1007/s11665-022-06736-1

Mat, M. F., Manurung, Y. H. P., Muhammad, N., Ditler, A., Abd Ghani, M. S., & Leitner, M. (2020). Grain growth prediction of bead-on-plate with filler wire SS316L using FEM. IOP Conference Series: Materials Science and Engineering (p. 012009). Purpose-LED Publishing. https://doi.org/10.1088/1757-899X/834/1/012009

Nazir, A., Gokcekaya, O., Md Masum Billah, K., Ertugrul, O., Jiang, J., Sun, J., & Hussain, S. (2023). Multi-material additive manufacturing: A systematic review of design, properties, applications, challenges, and 3D printing of materials and cellular metamaterials. Materials and Design, 226, 111661. https://doi.org/10.1016/j.matdes.2023.111661

Ning, J., Praniewicz, M., Wang, W., Dobbs, J. R., & Liang, S. Y. (2020). Analytical modeling of part distortion in metal additive manufacturing. International Journal of Advanced Manufacturing Technology, 107(1–2), 49–57. https://doi.org/10.1007/s00170-020-05065-8

Novelino, A. L. B., Carvalho, G. C., & Ziberov, M. (2022). Influence of WAAM-CMT deposition parameters on wall geometry. Advances in Industrial and Manufacturing Engineering, 5, 100105. https://doi.org/10.1016/j.aime.2022.100105

Prajadhiana, K. P., Taufek, T., Wan Abdul Rahaman, W. E., Manurung, Y. H. P., Adenan, M. S., Mat, M. F., Mohamad Fuzi, M. F. A., Mohammed Nasir, M. A., Mohamed, M. A., Jamaludin, M. F., & Triyono. (2023). Distortion analysis method for wire arc additive manufacturing component using thermomechanical computation with enhanced separation and deposition algorithm. 3D Printing and Additive Manufacturing, 11(4), 1616-1628. https://doi.org/10.1089/3dp.2023.0033

Reed, R. C., & Rae, C. M. F. (2014). Physical metallurgy of the Nickel-based superalloys. In D.E. Laughlin, & K. Hono (Eds.), Physical Metallurgy: Fifth Edition (pp. 2215-2290). Elsevier. https://doi.org/10.1016/B978-0-444-53770-6.00022-8

Special Metals Corporation. (2021). Special Metals Inconel G-3 Alloy. Alloy Digest, 70(8), Ni-774. https://doi.org/10.31399/asm.ad.ni0774

Taufek, T., Manurung, Y. H. P., Akma, S., Wan Abdul Rahaman, W. E., Irwan, M. H., Mohd Salleh, N. A., Adenan, M. S., Sahari, M. M., Chang, B., & Awiszus, B. (2022). Distortion analysis of generatively designed hinge bracket using meso-scaled thermomechanical simulation with experimental validation. Virtual and Physical Prototyping, 17(4), 966–988. https://doi.org/10.1080/17452759.2022.2092760

Wacker, C., Köhler, M., David, M., Aschersleben, F., Gabriel, F., Hensel, J., Dilger, K., & Dröder, K. (2021). Geometry and distortion prediction of multiple layers for wire arc additive manufacturing with artificial neural networks. Applied Sciences, 11(10), 4694. https://doi.org/10.3390/app11104694

Wolff, S. J., Gan, Z., Lin, S., Bennett, J. L., Yan, W., Hyatt, G., Ehmann, K. F., Wagner, G. J., Liu, W. K., & Cao, J. (2019). Experimentally validated predictions of thermal history and microhardness in laser-deposited Inconel 718 on carbon steel. Additive Manufacturing, 27, 540–551. https://doi.org/10.1016/j.addma.2019.03.019

Yakout, M., Elbestawi, M. A., Veldhuis, S. C., & Nangle-Smith, S. (2020). Influence of thermal properties on residual stresses in SLM of aerospace alloys. Rapid Prototyping Journal, 26(1), 213–222. https://doi.org/10.1108/RPJ-03-2019-0065

https://doi.org/10.24191/jmeche.v22i1.2801